Menopause: The Journal of The North American Menopause Society
Vol. 26, No. 11, pp. 000-000
DOI: 10.1097/GME.0000000000001395

The histological microstructure and in vitro mechanical properties of pregnant and postmenopausal ewe perineal body

Petra Kochová, PhD,[1] Lucie Hympánová, MD, PhD,[2,3,4] Rita Rynkevic, PhD Student,[2,3,5] Robert Cimrman, PhD,[1] Zbyněk Tonar, MD, PhD,[1] Jan Deprest, MD, PhD,[2,3,6] and Vladimir Kalis, MD, PhD[7,8]

Abstract

Objective: The mechanical properties and microstructure of the perineal body are important for the improvement of numerical models of pelvic organs. We determined the mechanical parameters and volume fractions of the ewe perineal body as an animal model.

Methods: The 39 specimens of 13 pregnant swifter ewes delivering by cesarean section (aged 2 years, weight 61.2 ± 6.2 kg (mean ± standard deviation) and 24 specimens of 8 postmenopausal swifter ewes 150 days after surgical ovariectomy (aged 7 years, 58.6 ± 4.6 kg)) were loaded uniaxially to determine Young's moduli of elasticity in the small (E_0) and large (E_1) deformation regions, and ultimate stresses and strains. The 63 adjacent tissue samples were processed histologically to assess volume fractions of smooth and skeletal muscle, adipose cells, elastin, and type I collagen using a stereological point testing grid. We compared the structural and mechanical differences along the ewe perineal body, and between pregnant and postmenopausal groups.

Results: The pregnant/postmenopausal perineal body was composed of smooth muscle (12/14%; median), skeletal muscle (12/16%), collagen (10/23%), elastin (8/7%), and adipose cells (6/6%). The E_0 was 37/11 kPa (median), E_1 was 0.97/1.04 MPa, ultimate stress was 0.55/0.59 MPa, and ultimate strain was 0.90/0.87 for pregnant/postmenopausal perineal body. The perineal body showed a structural and mechanical stability across the sites. The pregnant ewes had a higher amount of skeletal muscle, higher E_0, and a less amount of collagen when compared with postmenopausal ewes.

Conclusions: The data can be used as input for models simulating vaginal delivery, pelvic floor prolapsed, or dysfunction.

Key Words: Histology – Perineal body – Sheep – Ultimate strain – Ultimate stress – Volume fraction – Young's modulus of elasticity.

The perineum is a complex structure composed of a collagen and elastin network, and skeletal and smooth muscles. It is located in the midline between the posterior fourchette and the anal sphincter. A key component of perineum is the perineal body (known also as the central perineal tendon) connected to the perineal membrane serving as the site of attachment of many structures.[1] It has an irreplaceable function in the complex interaction of the pelvic floor muscles and connective tissue, and is crucial for the support, especially of the lower part of the vagina, and protects the anal sphincter during vaginal delivery. The perineal body with its surrounding muscles and connective tissue collectively supports the distal vagina, and anal canal.[2] Damage of active or passive components of these structures can lead to a perineal descent, a gaping genital introitus, and a posterior vaginal wall prolapse.[3] Either a detachment of the perineal body from the perineal membrane, or a tear along the rectovaginal septum, bulbocavernosus muscles, superficial and deep transverse perineal muscles, and external anal sphincter muscles, may lead to a descent of the perineal body

Received May 3, 2019; revised and accepted June 5, 2019.

From the [1]European Centre of Excellence NTIS, Faculty of Applied Sciences, University of West Bohemia, Pilsen, Czech Republic; [2]Centre for Surgical Technologies, KU Leuven, Leuven, Belgium; [3]Department of Development and Regeneration, KU Leuven, Leuven, Belgium; [4]The Institute for the Care of Mother and Child, Third Faculty of Medicine, Charles University, Prague, Czech Republic; [5]INEGI, Faculdade de Engenharia da Universidade do Porto, Porto, Portugal; [6]Pelvic Floor Unit, University Hospitals KU Leuven, Leuven, Belgium; [7]Biomedical Center, Faculty of Medicine, Charles University, Pilsen, Czech Republic; and [8]Department of Gynecology and Obstetrics, University Hospital, Pilsen, Czech Republic.

Funding/support: Project LO1506 of the Czech Ministry of Education, Youth and Sports under the program NPU I and from European Regional Development Fund-Project ''Application of Modern Technologies in Medicine and Industry'' (No. CZ.02.1.01/0.0/0.0/17_048/0007280) and Charles University Research Fund (Progress Q39).

Financial disclosure/conflicts of interest: None reported.

Supplemental digital content is available for this article. Direct URL citations appear in the printed text and are provided in the HTML and PDF versions of this article on the journal's Website (www.menopause.org).

Address correspondence to: Petra Kochová, PhD, European Centre of Excellence NTIS, Faculty of Applied Sciences, University of West Bohemia, Technická 2967/14, 306 14 Pilsen, Czech Republic. E-mail: kochovap@ntc.zcu.cz

below the level of the ischial tuberosities and can contribute to defecatory and sexual dysfunctions.[4] The loss of a fibromuscular support of the pelvic organs leads to the pelvic organ prolapse (POP), that is, to a vaginal protrusion and the descent of the pelvic organs into and out of the vaginal canal.[5]

The mechanical properties of the perineal body significantly influence the mechanics of the surrounding tissues. The pubovisceral muscle enthesis and the perineal body are the regions of the greatest strain during vaginal delivery.[6] This strain places these regions at the highest risk of a stretch-related injury. The decrease of the perineal body stiffness by 40%, 50%, and 60% led to reductions in the maximum principal stretch ratio for the pubovisceral muscle enthesis of 8%, 13%, and 18%, respectively, and therefore reduced the risk of injury.[6]

The modeling of the pelvic floor structures has recently been found useful in the analysis and evaluation of pathophysiological processes and the execution of obstetric procedures that would otherwise have been very complicated or even impossible, and might lead to a better understanding of prolapse pathophysiology. Many studies have predominantly evaluated the stretching and/or subsequent pubovisceral muscle injury during vaginal birth.[6-9] Other studies described finite element models of vaginal delivery itself.[7,10-13] Further modeling references include models of the female pelvic system,[14] pathological dysfunctions, development of POP,[12,15-18] supporting mesh insertion, and reconstructive surgery.[5,19,20] Most of the models include vagina, rectum, bladder, and ligaments, and no perineal body. In all computational models, the right choice of a constitutive model, its geometry, and mechanical parameters is crucial.[8,21]

One of the main limitations of perineal body modeling is the absence of knowledge of real biomechanical parameters. Material data based on experiments on the perineal body are rare.[22-24] The mechanical testing is devoted mostly to the deep structures of the pelvic floor, that is, uterus, cervix, vagina, and pelvic ligaments.[25] The mechanical parameters of the pelvic floor muscles (pubovisceral muscle, illiococcygeal muscle, and the perineal body) are for modeling purposes commonly substituted by parameters of other muscles, namely the tongue muscle,[26] skeletal muscle,[10] and cardiac muscle.[7,11,20]

Thus, there exist only a few mechanical studies on human cadaver specimens of the perineal body.[22,27] Note that due to ethical reasons it is practically impossible to study material properties of the human perineal body within the prenatal period or during pregnancy. Animal models, such as rodents, rabbits, nonhuman primates, or sheep are commonly used for mechanical measurements of pelvic floor components.[28,29] The adult ewe is a large-animal model with a suitable size and anatomical structure.[28,30] The pelvic connective tissue anatomy of the sheep is similar to that of humans with three levels of support.[30] Moreover, they spontaneously develop POP related to pregnancy and vaginal birth, and can be used for vaginal surgery training. We used the perineal body of pregnant ewes during delivery by caesaran section and postmenopausal ewes 150 days after ovariectomy.

Knowledge of the structure and mechanics of the perineal body is helpful to control the vaginal delivery process, and/or subsequently, it also improves a clinician's ability to identify defect(s) in the pelvic support, and facilitates a better diagnosis and treatment of POP. The tissue function is related to its structure and mechanical properties. Therefore, we decided to analyze the components and in vitro mechanical parameters of the perineal body to improve the current perineal models,[13,31] and increase the precision of future mathematical simulations.

The main aims of the study were:

1. to assess the volume fractions of smooth muscle, skeletal muscle, collagen, elastin, and adipose tissues along the perineal body (in three regions of the perineal body);
2. to determine the Young's moduli of elasticity in the small and large deformation regions, the ultimate stress, and the ultimate strain along the perineal body (in the regions of the perineal body);
3. to find differences between structural and mechanical parameters of the ewe perineal tissue during pregnancy and after menopause;
4. to test correlations between the volume fractions of major perineal tissue constituents and mechanical properties of the perineal body.

METHODS

Specimen collection and preparation

Thirteen swifter ewes delivered by cesarean section (group pregnant (PREG), 2 years old, second delivery, weight 61.2 ± 6.2 kg [mean $\pm$ standard deviation]) and eight swifter ewes 150 days after surgical ovariectomy (group postmenopausal (POST), 7 years old, more than four deliveries, mean weight 58.6 ± 4.6 kg [mean $\pm$ standard deviation]) were used for the study. The ewes were euthanized by intravenous administration of pentobarbital (Release, Ecuphar, Oostkamp, Belgium; 20 mL/50 kg). The full perineal area between rectum and vagina was excised. The skin and the subcutaneous tissue were removed to keep only the fibromuscular layer of the central tendon. Tissue was divided into three regions of the perineal body: at midline region (R2), and in the sagittal section 5 mm left (R1) and 5 mm right (R3) (anatomic orientation) from the midline (Fig. 1).

In total 63 specimens (39 group PREG, 24 group POST) were used for the mechanical measurement to obtain the mechanical parameters and 63 neighboring specimens were used for the histological analysis to assess the structural parameters of the perineal body.

A deep freezing conservation (-20°C) was applied to the specimens used for the mechanical testing immediately after the collection. The observation that the passive mechanical properties of dead tissue are unaltered during the freezing process has been reported for various kinds of other tissues (ligament, tendon, adipose tissue, arterial tissue, ovine vaginal tissue).[32-36]

For the mechanical and also structural analysis, we followed our protocol published earlier.[27]

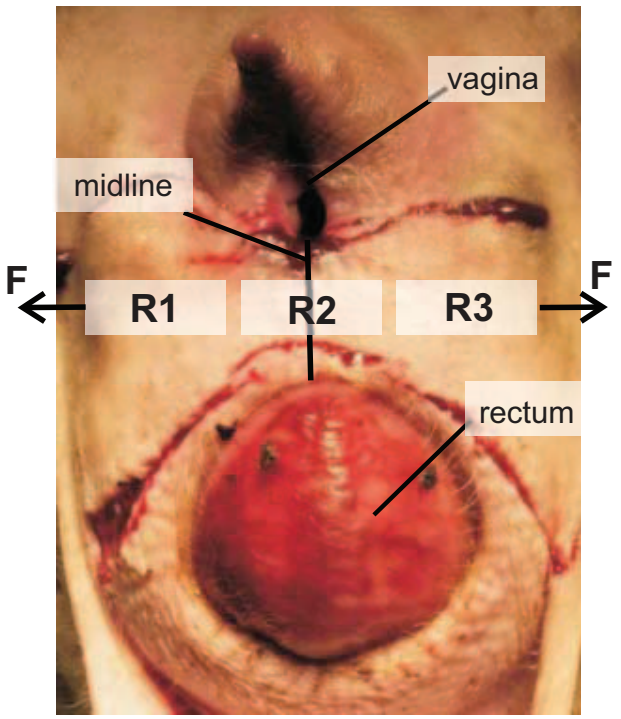

FIG. 1. The excision of specimens from the ewe perineal body symmetrically to the midline. The region R2 was the region of midline. The regions R1 was cut in the sagittal section 5 mm right (anatomic orientation) and R3 was cut in the sagittal section 5 mm left (anatomic orientation) from the midline. The mechanical loading was applied perpendicular to the midline (F).

Histology

The tissue was put into formalin immediately after separating from the body, and after that it underwent histological processing. Specimens were perfused with 10% buffered formalin and embedded in paraffin. No pressure was used during the fixation procedure. Each tissue block was then cut using a Leica RM 2135 microtome (Leica Microsystems GmbH, Wetzlar, Germany) into vertical uniform random serial sections with a thickness of 5 μm.[37] The sections were then stained using a combination of three methods: Verhoeff's hematoxylin and green trichrome, orcein stain, and picrosirius red.

Microscopic quantification

We quantified five parameters: the volume fractions of skeletal muscle, smooth muscle, elastin, type I collagen, and adipose cells in three regions (R1, R2, R3) of the ewe perineal body. Structures not belonging to any of these (eg, lumina of blood vessels, peripheral nerves, fibroblasts, and fibrocytes) were considered as residual tissue, the volume of which was calculated as 1 minus the sum of the quantified volume fractions. The Ellipse 3D software package (ViDiTo, Inc. Košice, Slovak Republic) including the standard stereological methods was used for this quantification.

The Verhoeff's hematoxylin and green trichrome were used for the smooth and skeletal muscle quantification (Fig. 2A). The orcein staining was used for the elastin and adipose cells quantification (Fig. 2B). The picrosirius red staining in polarized light was used for the type I collagen quantification (Fig. 2C and D). We used 186 sections in total for the quantification. Each section was uniformly captured on 10 to 12 micrographs using an Olympus BX52 microscope with a 10× objective.

The standardized and established stereological methods commonly used for quantification of inner structures of tissues and organs were used for the quantification.[37,38] The volume fractions of individual components were determined using the Cavalieri principle: the number of intersections between the point test grid and the component of interest were divided by the total number of test grid points.[37,38] The total number of intersections between objects and the test point grid was 30,458. The histological quantification was performed by a single observer (P.K.). There was no interobserver and a low intraobserver variability (see details in Supplementary material 1, http://links.lww.com/MENO/A444).

Note that the type I collagen volume fraction included the free collagen, and also the collagen of the adventitia of the blood vessels.

Mechanical measurements

The frozen specimens were kept at room temperature to thaw out for a period of 6 hours before the mechanical measurement. The specimens were then clamped into the measurement device. The thickness of specimens was about 2.5 mm and the width of specimens was about 10.5 mm. The thickness and width of specimens were measured by digital calipers in the relaxed state of the tissue by a single person (R.R.) to avoid varying tissue compression during measurements. Each whole specimen was put between the caliper jaws to measure the thickness and the width of the specimen. During the measurement the caliper jaws just touched the whole specimen without any visible deformation. The initial length (transversal direction) of each specimen between the clamps was preset to 10 mm. The uniaxial tensile loading was applied perpendicularly to the midline of the perineal body. The traction machine Zwick/Roell Z050 (Zwick/Roell, Ulm, Germany) was used for the mechanical testing. The mechanical tests were performed at room temperature.

Each specimen was preconditioned using 20 cycles with a linearly increasing and decreasing elongation of up to 15% of the initial length. After this preconditioning, a linear increase in loading was applied until the perineal body ruptured (Fig. 3). The loading velocity was 6 mm/min.[22,27] The applied deformation and measured forces were recorded during the testing to obtain a stress-strain curve which was used to determine the mechanical properties of the perineal body, that is, the Young's moduli of elasticity, ultimate stress, and ultimate strain. The Young's modulus of elasticity was defined as the slope of the stress-strain curve, and is measured in Pa (kg/ms^2) (Fig. 3A). The stress corresponds to the force acting on an area of a deformable tissue. The strain is the ratio of the change in length caused by the stress to the original dimension of the specimen. The stress was defined as the

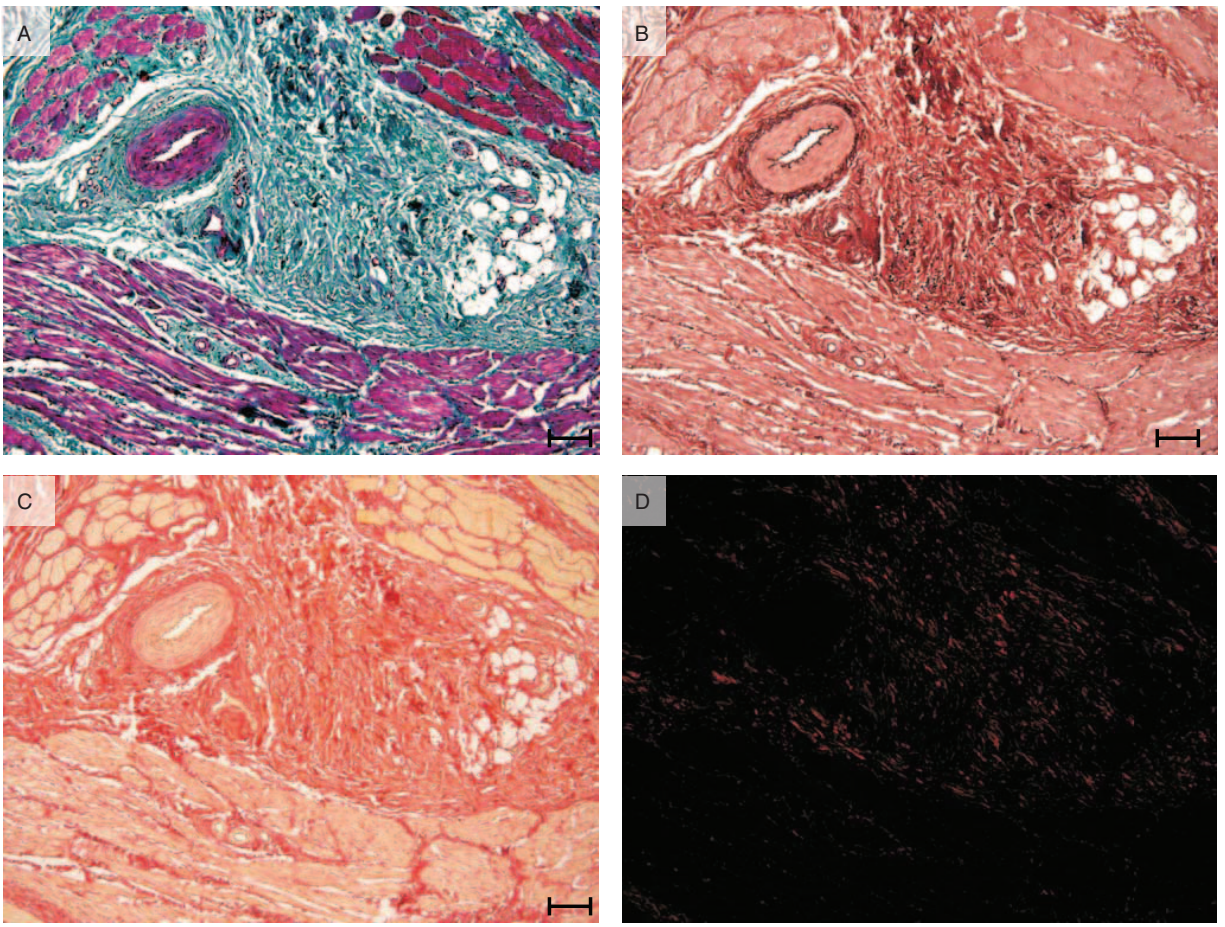

FIG. 2. The histological staining of slices from the same ewe perineal body specimen: Verhoeff's hematoxylin and green trichrome showing the contrast between connective tissue (green) and muscle (reddish) tissue (**A**). Orcein staining used for visualization of elastin (dark brown) (**B**), Picrosirius red staining in bright field (**C**), and under polarized light (**D**), showing type I collagen (reddish to yellow). Scale bars = 100 μm.

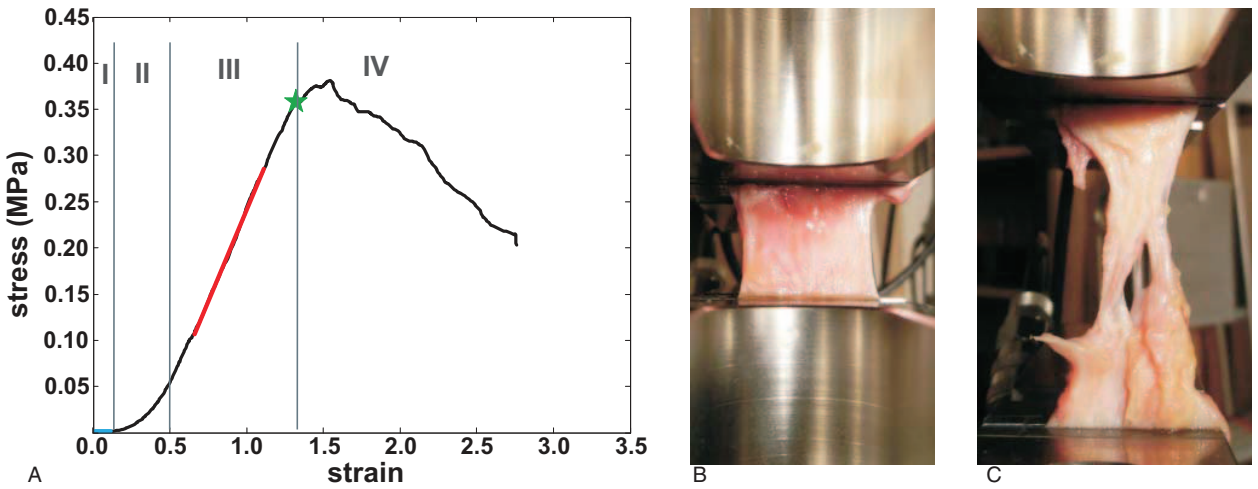

FIG. 3. (**A**) An example of the nonlinear stress-strain curve of the midline region of the ewe perineal body. I—the small deformation region with a low stiffness (Young's modulus of elasticity, slope of the curve, blue line); II—the region of tissue stiffening; III—the linear large deformation region with a high stiffness (Young's modulus of elasticity, red line); IV—the region preceding tissue rupture with initialization of the rupture (green star) after rupturing of individual components of the tissue. (**B, C**) A specimen in the measurement device during the test. The tissue rupture due to mechanical loading is visible (**C**).

actual force divided by the area of the initial cross-section (width × thickness dimension) of the specimen. The strain was defined as the elongation of the tissue divided by its initial length. Given the stress-strain curve, the least-squares method was used to determine the Young's moduli in the small deformation region (0%-18%, depending on the shape of the stress-strain curve) and in the large deformation region (20%-150%, depending on the shape of the stress-strain curve) (Fig. 3). All mechanical parameters were determined using the open source software Elfpy (https://github.com/rc/elfpy).

In the present study, the ultimate stress and the ultimate strain were determined at the starting point of the perineal body rupture, which is not necessarily at the point of the highest stress of the stress-strain curve (Fig. 3).

Statistical analysis

The normality of the volume fractions and mechanical parameters was tested using the Shapiro-Wilk's *W* test. All the statistical tests are nonparametric methods because some data sets did not pass the test for normality. Statistica software (version 8.0, Statsoft, Inc., Tulsa, OK) was used for the statistical analysis. The differences of structural and mechanical parameters between regions (R1, R2, R3) were analyzed using the Friedman analysis of variance (ANOVA) test. The Friedman ANOVA test found significant differences between regions only for the skeletal tissue volume fraction in group POST and in Young's moduli of elasticity. Thus the post hoc multiple comparisons using the Wilcoxon matched-pairs test were then performed only for these parameters. The differences of structural and mechanical parameters between groups (group PREG, group POST) were analyzed using the Mann-Whitney *U* test. The correlation between structural and mechanical parameters was analyzed using the Spearman rank *r* correlation coefficient (level of significance 0.05). The average volume fractions for each component from all three perineal regions of group PREG and group POST were calculated and then used in the Mann-Whitney *U* test and correlation analysis. The effect size was evaluated as $\eta 2$ and d_{cohen} values using the effect size calculator for nonparametric tests (https://www.psychometrica.de/effect_size.html#nonparametric).

RESULTS

The morphometric data are in the form of continuous variables provided in Supplementary material 2 (http://links.lww.com/MENO/A445).

Microscopic quantification

The ewe perineal body is composed of type I collagen and elastin fibers, bundles of smooth muscle cells, skeletal muscle fibers, adipose tissue, blood vessels, peripheral nerves, fibroblasts, fibrocytes, and other cells occurring in the collagen fibrous tissue (Fig. 4). The skeletal and smooth muscle bundles were often close together (Fig. 4A) and embedded in collagen tissue (Fig. 4A–C). The collagen surrounded the smooth or skeletal muscles (Fig. 4A, B) or created dense wavy bundles (Fig. 4C). The elastin was present in the areas around or between adipose cells (Fig. 4E, F) or in the dense connective tissue (Fig. 4D). The adipose cells were grouped in clusters surrounded by or crossed by collagen and elastin fibers (Fig. 4E) or individually occurring within connective tissue (Fig. 4D, F).

Volume fractions along the ewe perineal body

The volume fractions of skeletal muscle, smooth muscle, collagen type I, elastin, and adipose tissue are shown in Table 1 and Fig. 5. The Friedman ANOVA test showed differences only in the skeletal muscle fibers content ($P = 0.02$) between regions of postmenopausal ewes (group POST). The Wilcoxon matched-pairs test showed only differences between the skeletal muscle content in the midline region R2 compared with region R1 ($P = 0.03$). The midline region R2 had a higher amount of skeletal muscle than region R1.

The smooth muscle cells were the most abundant tissue in pregnant ewes (0.07-0.15, interval of medians of individual regions), followed by skeletal muscles (0.05-0.15), and type I collagen fibers (0.08-0.12). Lower volume fractions were occupied by the elastin fibers (0.07-0.09) and adipose cells (0.06).

In ovariectomized ewes (group POST), the highest volume was occupied by type I collagen fibers with volume fractions (0.20-0.25), followed by smooth muscle (0.1-0.15), elastin fibers (0.05-0.08), and adipose cells (0.04-0.07). The volume fraction of the skeletal muscle fibers in this group was less than 0.05.

The residual tissue in both ewe groups was composed mostly of peripheral nerves, lumina of blood vessels, fibroblasts, and fibrocytes (Fig. 4G, H).

Structural differences between group PREG and group POST of the ewe perineal body

The Friedman ANOVA test showed only minimal differences between the volume fractions along the ewe perineal body in both groups; thus the average volume fractions for each component from all three perineal regions were calculated and then used for the Mann-Whitney *U* test. The group PREG had a higher amount of skeletal muscle ($P < 0.001$) and a lower amount of type I collagen ($P < 0.001$) than the group POST.

Mechanical measurements

The stress-strain curves of the perineal bodies showed similar shapes in all tested tissue specimens (Fig. 3). The curves were nonlinear and consisted of a region of small deformation (0%-18%) with a low stiffness, followed by a region of stiffening, and then a linear region of large deformations (20%-150%) with an increased stiffness.

The mechanical properties are summarized in Table 2 and Fig. 6. The Young's modulus of elasticity in the small deformation region was 20 to 50 kPa (interval of medians

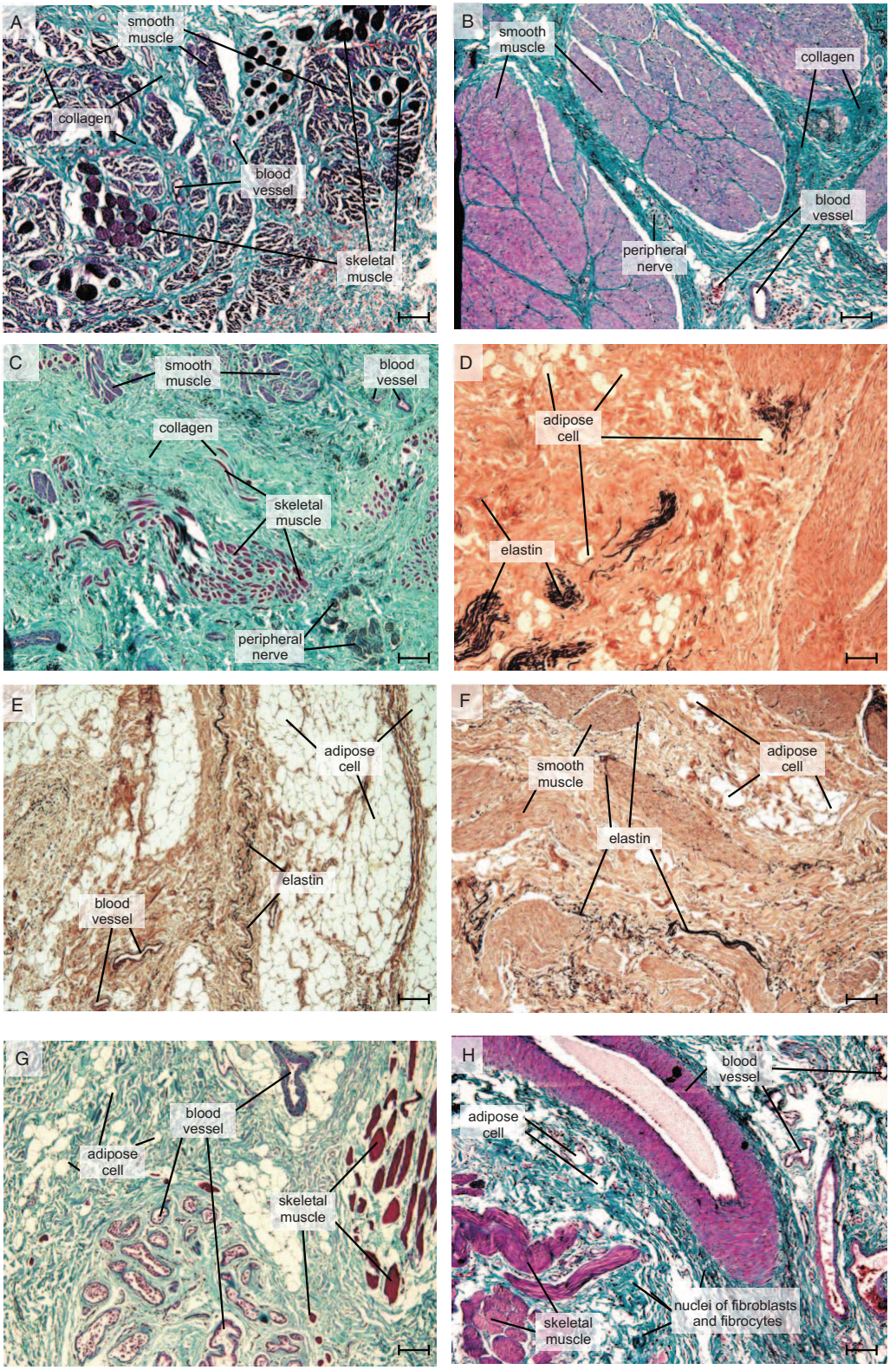

FIG. 4. The structure of the ewe perineal body: the skeletal and smooth muscle bundles were embedded in collagen tissue (**A-C**), the bundles of skeletal and smooth muscle were often close together (**A**), the elastin was presented in the areas around or between adipose cells (**E, F**) or in the dense connective tissue (**D**), the adipose cells were grouped in clusters surrounded by or crossed by collagen and elastin fibers (**E**) or individually pasted in connective tissue (**D, F**). The residual tissue was composed of blood vessels, peripheral nerves cells, fibroblasts, and fibrocytes. Verhoeff's hematoxylin and green trichrome (**A-C, G, H**), orcein staining (**D-F**). The scale bar = 100 μm.

TABLE 1. *The volume fractions of the smooth muscle tissue, skeletal muscle tissue, collagen, elastin, adipose tissue, and residual tissue (neural cells, blood vessels lumina, fibrocytes, and fibroblasts) along the perineal body of pregnant ewes (group PREG) and ewes after ovariectomy (group POST) (regions R1-R3)*

	Group PREG			Group POST		
Component	R1	R2	R3	R1	R2	R3
Smooth muscle	0.12 (0.04-0.15)	0.15 (0.01-0.22)	0.08 (0.03-0.16)	0.15 (0.08-0.17)	0.13 (0.07-0.24)	0.11 (0.05-0.17)
Skeletal muscle	0.15 (0.11-0.17)	0.05 (0.01-0.26)	0.10 (0.04-0.18)	0.05 (0.00-0.10)	0.001 (0.00-0.02)	0.03 (0.01-0.06)
Collagen	0.08 (0.07-0.13)	0.10 (0.07-0.33)	0.12 (0.09-0.15)	0.20 (0.17-0.24)	0.23 (0.21-0.27)	0.25 (0.18-0.28)
Elastin	0.09 (0.06-0.09)	0.07 (0.04-0.11)	0.08 (0.07-0.09)	0.05 (0.05-0.07)	0.09 (0.07-0.10)	0.07 (0.05-0.08)
Adipose cells	0.06 (0.04-0.08)	0.06 (0.05-0.07)	0.06 (0.04-0.09)	0.07 (0.05-0.10)	0.04 (0.03-0.07)	0.07 (0.04-0.11)
Residual tissue	0.47 (0.24-0.59)	0.45 (0.13-0.51)	0.47 (0.42-0.54)	0.48 (0.45-0.53)	0.49 (0.38-0.54)	0.49 (0.44-0.52)

Given as the median (interquantile range). The number of investigated specimens was 39 (13 per region) in group PREG (pregnant ewes) and 24 (8 per region) in group POST (postmenopausal ewes).
R1, in the sagittal section 5 mm left from the midline; R2, midline region; R3, in the sagittal section 5 mm right from the midline.

of individual regions) in the group PREG and 10 to 16 kPa in the group POST. The Young's modulus of elasticity in the large deformation region was 0.9 to 1.0 MPa in group PREG and 0.8 to 1.6 MPa in group POST. The considerable stiffening of the perineal body with increasing strain was clearly visible from the curves. The ultimate strain was 0.8 to 1.0 in the group PREG and 0.7 to 1.0 in the group POST, and the related ultimate stress was 0.5 to 0.6 MPa in group PREG and 0.4 to 0.6 MPa in group POST.

Mechanical parameters along ewe perineal body

The determined mechanical parameters of the perineal tissue were similar in the all three investigated regions. An exception was the Young's modulus of elasticity in the small deformation region in group PREG ($P = 0.01$), where the stiffness was higher in region R3 when compared with other regions (R1: $P = 0.03$; R2: $P = 0.04$). The second exception near the level of significance was the Young's modulus of elasticity in the large deformation region ($P = 0.049$) in group POST, where the stiffness in region R2 was smaller than in region R1 ($P = 0.02$).

Mechanical differences between group PREG and group POST of the ewe perineal body

The Friedman ANOVA test showed only minimal differences between the mechanical parameters along the ewe perineal body in both groups; thus the averages from all three perineal regions were calculated and then used for the Mann-Whitney *U* test. The group PREG had a higher Young's modulus of elasticity in the small deformation region ($P < 0.01$) than the group POST.

Correlations between mechanical parameters and component content

Group PREG

The ultimate stress was positively correlated with the fraction of smooth muscle amount ($r = 0.33$). The ultimate strain was negatively correlated with the elastin amount ($r = -0.37$). The positive correlation was found between the Young's modulus of elasticity in the large deformation region and the ultimate stress ($r = 0.80$). The negative correlation was found between the ultimate strain and the Young's modulus in the small deformation region ($r = -0.46$). The amount of the smooth muscle showed a positive correlation with the elastin amount ($r = 0.42$) and a negative correlation with the skeletal muscle amount ($r = -0.62$).

Group POST

There was no correlation between the mechanical and structural properties. A positive correlation was between the Young's modulus of elasticity in the small and large deformation region ($r = 0.50$), and between the Young's modulus of elasticity in the large deformation region and the ultimate stress ($r = 0.76$). A negative correlation was found between the ultimate strain and the Young's moduli ($r = -0.52$ in the small deformation region, -0.71 in the large deformation region). The amount of adipose cells showed a positive correlation with the skeletal muscles amount ($r = 0.47$) and a negative correlation with the type I collagen ($r = -0.50$) and elastin ($r = -0.44$) amount, respectively.

The complete statistical analyses of the Friedman ANOVA test, Wilcoxon matched pair test, and Mann-Whitney *U* test is provided in Supplement 3 (http://links.lww.com/MENO/A446) and the complete correlation analysis is provided in Supplementary material 4 (http://links.lww.com/MENO/A447).

DISCUSSION

The results showed that the structural and mechanical parameters differ only slightly along the perineal body in both groups. The groups PREG and POST differ only in skeletal muscle and collagen amount, and in the initial stiffness given by the Young's modulus of elasticity in the small deformation region. It is also visible that the regions R1 and R3 had the mean values of components volume fractions, and also those of mechanical parameters closer to each other than to the region R2, with an exception of the Young's modulus E_0 in the small deformation region in group PREG.

Microscopic quantification

The microscopic structure of the ewe perineal body (Fig. 4) is similar to that of the human one.[27] The results show a structural similarity of the perineal body across the sites. The group PREG had a higher amount of skeletal muscle, but a smaller amount of type I collagen than the group POST, which

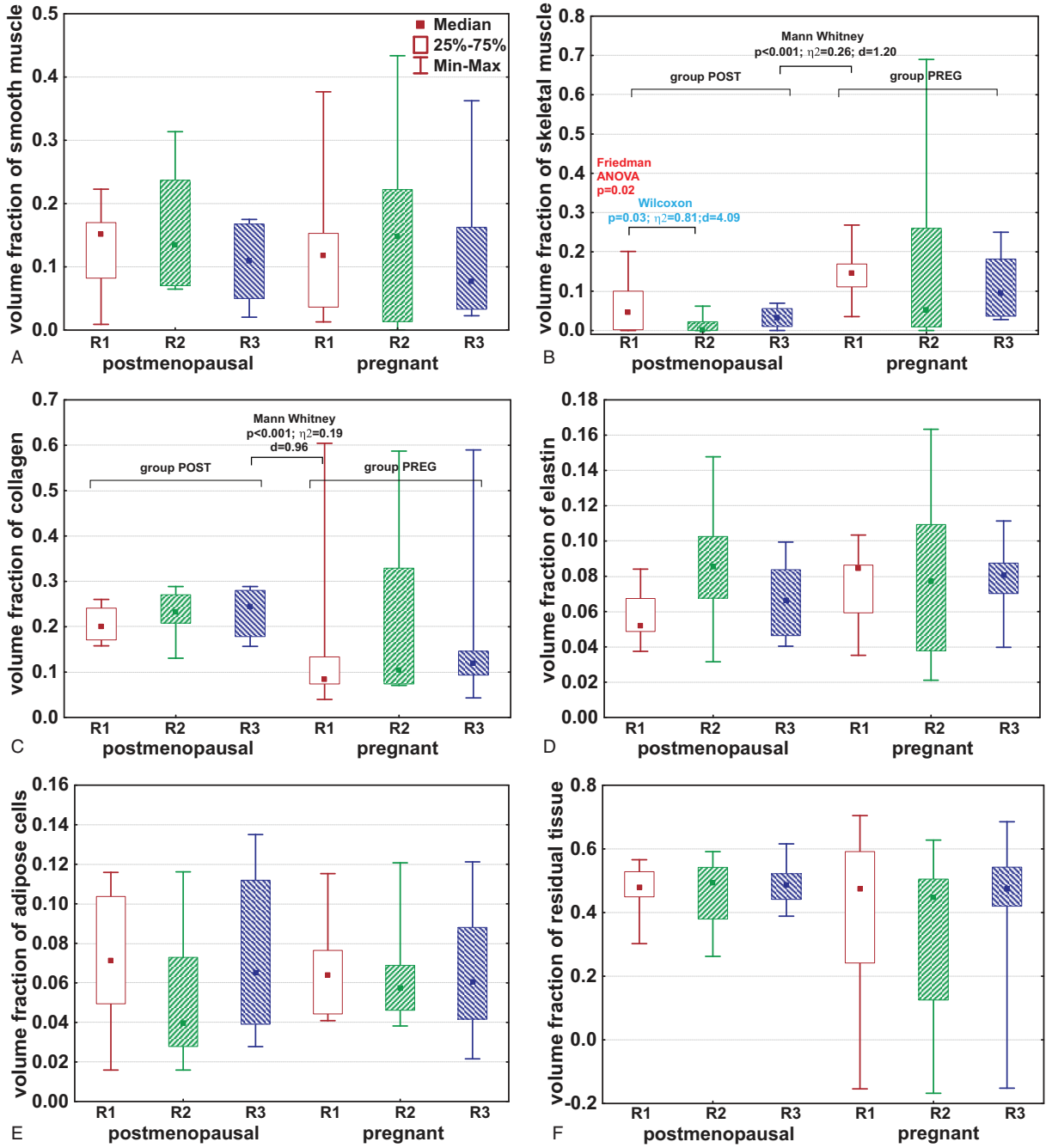

FIG. 5. The volume fractions of smooth muscle tissue (**A**), skeletal muscle tissue (**B**), collagen (**C**), elastin (**D**), adipose cells (**E**), and the residual tissue (**F**) along the pregnant and postmenopausal ewe perineal body (regions R1-R3). The number of investigated specimens was 39 in group PREG (pregnant ewes) and 24 in group POST (postmenopausal ewes). The square dot (■) denotes the median, the rectangle (□) spans the interquartile range, and the whiskers (—) denote the limit values. The differences between regions were tested by the Friedman ANOVA test and the Wilcoxon matched-pair test. The differences between groups were tested using the Mann-Whitney *U* test. The level of significance was 0.05. The effect size is given by $\eta 2$ and d_{cohen} values. The Friedman ANOVA test showed differences only in the skeletal muscle fibers content between regions of postmenopausal ewes (group POST). The Wilcoxon matched-pairs test showed that the midline region R2 had a higher amount of skeletal muscle then the region R1. The Mann-Whitney *U* test showed that the group PREG had a higher amount of skeletal muscle and a lower amount of type I collagen then the group POST. ANOVA, analysis of variance.

could be related to the differences in the initial stiffness between these groups discussed later.

The volume fractions of the main components of postmenopausal perineal ewe tissue were similar to those of postmenopausal human perineal body.[27]

The transverse muscles serve as a passive support to the perineal body.[39] The muscle fibers of the superficial and deep transverse perineal muscles pass from one perineal muscle to the other across the perineal body with a digastric pattern. Our results showed a similar muscular proportion in the

TABLE 2. *Mechanical parameters—the Young's modulus of elasticity in the small deformation region (E_0), the Young's modulus of elasticity in the large deformation region (E_1), the ultimate stress when the rupture occurred, the ultimate strain when the rupture occurred along the perineal body of pregnant ewes (group PREG), and ewes after ovariectomy (group POST) (regions R1-R3)*

	Group PREG			Group POST		
Parameter	R1	R2	R3	R1	R2	R3
E_0 (MPa)	0.02 (0.01-0.04)	0.03 (0.02-0.06)	0.05 (0.04-0.08)	0.01 (0.00-0.04)	0.01 (0.00-0.05)	0.02 (0.01-0.08)
E_1 (MPa)	0.99 (0.70-1.43)	1.00 (0.64-1.08)	0.93 (0.67-1.62)	0.82 (0.63-1.72)	0.92 (0.59-1.48)	1.63 (1.04-2.15)
Ultimate strain	0.89 (0.74-1.34)	1.13 (0.87-1.05)	0.84 (0.82-1.05)	0.78 (0.53-1.17)	1.04 (0.75-1.24)	0.73 (0.57-1.00)
Ultimate stress (MPa)	0.53 (0.45-0.66)	0.58 (0.31-0.71)	0.58 (0.41-0.83)	0.41 (0.26-0.65)	0.53 (0.40-0.71)	0.61 (0.57-0.78)

Given as the median (interquantile range). The number of investigated specimens was 39 (13 per region) in group PREG (pregnant ewes) and 24 (8 per region) in group POST (postmenopausal ewes).
R1, in the sagittal section 5 mm left from the midline; R2, midline region; R3, in the sagittal section 5 mm right from the midline.

midline region R2 as in the laterally located R1 and R3 regions with an exception of the skeletal muscle content in the group POST, where the midline region R2 had a higher amount of skeletal muscle than the region R1. This difference could support the concept of a digastric insertion of the muscle in the midline region.[39] The digastric pattern permits simultaneous contraction of the muscles on both sides as a single unit. The perineal muscle contraction protects the perineum against increased intra-abdominal pressure and perineal descent.

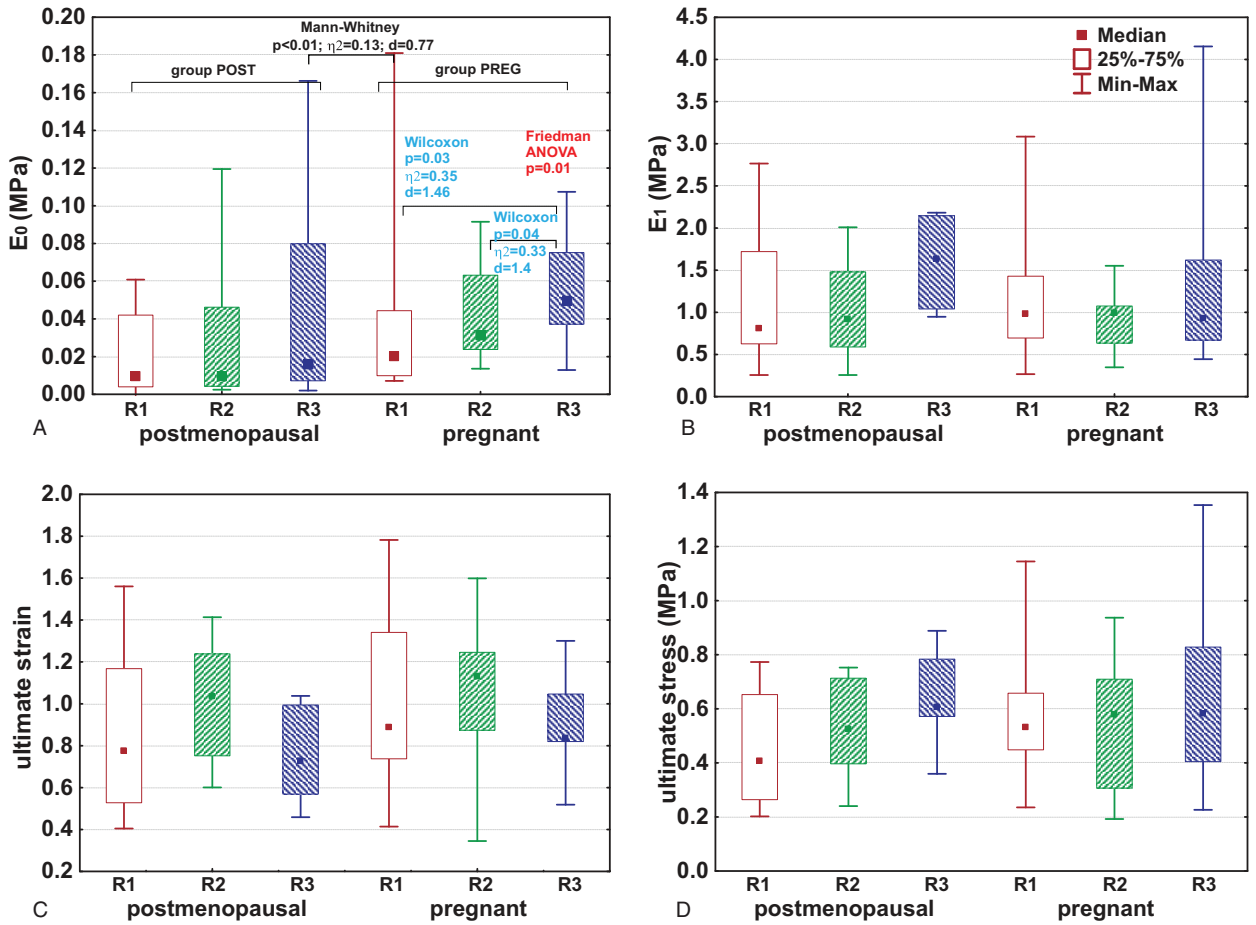

FIG. 6. The mechanical parameters of pregnant and postmenopausal ewe perineal body. (**A**) E_0, the Young's modulus of elasticity in the small deformation region. (**B**) E_1, the Young's modulus of elasticity in the large deformation region. (**C**) The ultimate stress when the rupture occurred. (**D**) The ultimate strain when the rupture occurred. The number of investigated specimens was 39 in group PREG (pregnant ewes) and 24 in group POST (postmenopausal ewes). The square dot (■) denotes the median, the rectangle (□) spans the interquartile range, and whiskers (=) denote the limit values. The differences between regions were tested by the Friedman ANOVA test and the Wilcoxon matched-pair test. The differences between groups were tested using the Mann-Whitney *U* test. The level of significance was 0.05. The effect size is given by η2 and d_{cohen} values. The Young's modulus of elasticity in the small deformation region in group PREG was higher in region R3 when compared with other regions. The Young's modulus of elasticity in the large deformation region in group POST was smaller in region R2 than in region R1. The Mann-Whitney *U* test showed that the group PREG had a higher Young's modulus of elasticity in the small deformation range than the group POST.

The anatomy and histology of the perineal body is also highly relevant to the effectiveness of pelvic floor training,[40] nonsurgical and surgical pelvic floor treatments,[5] and to a surgical oncological approach in patients undergoing surgery for low rectal cancer.[41]

Mechanical measurements

The results showed that the ewe perineal body, similarly to the human one,[27] was a viscoelastic material. The response on mechanical loading of such a material is the combination of a pure elasticity, where the material, after deformation caused by loading, returns to its original shape after unloading, and viscosity, which is a resistance of a material to a rate of deformation. This behavior is connected with hysteresis,[28,42] where during a cyclic loading, the unloading stress-strain curve does not follow the loading curve exactly, but remains below the loading curve, meaning that an energy dissipation occurs. The hysteresis was observed in our study during preconditioning. In our case, after more than 10 cycles of the initial cyclic loading and unloading, the loading and unloading stress-strain curves began to follow, repeatedly, the loading and unloading stress-strain curves of previous cycles. This state was defined as the endpoint of preconditioning (20 cycles), after which the tensile test with the linearly increasing loading could be started, continuing until tissue rupture.

The ewe perineal body exhibited a nonlinear stress versus strain relation: at the low loading levels it had a low stiffness, which rapidly increased at the high loading levels above 20% (depending on the specimen) (Fig. 3). Collagen crimping appears to play an important role in the perineum as in any organ containing collagen. The collagen fibers provide the resistance to external mechanical tensile forces and are responsible for the material tensile strength.[43] The collagen fibers are initially (at low deformations) crimped. And they become gradually straight during the stretching (tissue elongation). In the initial phase of loading, the material properties of collagen only marginally influence the modulus of elasticity of the overall tissue. After stretching, collagen fibers with their high Young's modulus of elasticity (1-2.5 GPa for collagen in rat-tail tendon[19]) begin to contribute to the total mechanical response of the tissue.[44] This is connected with the tissue stiffening during an increasing loading and with a high stiffness in the large deformation region. The tissue response during small deformations is given mostly by the elastin fibers (with the Young's modulus of elasticity 0.6 MPa[45]). The main function of elastin fibers is to hold the arrangement of the extracellular matrix and to return the tissue to its original shape after unloading. The muscles (with the Young's modulus of elasticity 4-150 kPa in the relaxed state[46-50] and 32 kPa to 20 MPa in the active state[46,48,49]) provide the passive and active mechanical support to the tissue during a low, and also a high mechanical loading.

We found a difference between pregnant and postmenopausal ewe groups only during the low mechanical loading, where the pregnant ewes had a higher stiffness. The mechanical properties of the tissue are given by composition and arrangement of its components, and by their mechanical properties. The stiffness differences between groups could be thus connected with the finding that the perineal body of pregnant ewes had a higher amount of skeletal muscle.

The information on mechanical properties of the perineal body in the literature is scarce.[23,22,27] The ultimate strain of 0.98 for pregnant and 1.75 for postmenopausal ewes, respectively, are similar to values obtained for the human perineal body (pregnant 1.78,[22] and postmenopausal 1.40[27]). The Young's modulus of elasticity in the small deformation region of postmenopausal ewe perineal body (11 kPa) was similar to the human postmenopausal one (18 kPa).[27] The obtained ultimate stress of 0.58 and 0.63 MPa (pregnant and postmenopausal ewes) is much lower than that obtained by Jing (10 MPa).[22] This difference could be explained by Jing's loading of the perineal body along the direction of the fibers,[22] while we loaded the tissue with various orientations to the fibers uniaxially and strictly transversally with respect to the midline of the perineum (Fig. 1). The direction of loading in the present study imitates the physiological loading of the perineum during a spontaneous vaginal delivery.[51] The ewe perineal body after ovariectomy had a higher Young's modulus of elasticity in the large deformation region (four times) and ultimate stress (three times) than the human postmenopausal perineal body.[27]

Data on the biomechanical properties of the pelvic tissues are hard to mutually compare due to variation in animal models, definition of specimens' location, testing protocols, clinical data (age), and constitutive models.[22,25,52-56] For example, the preconditioning and loading velocity are very important factors of testing protocols. The preconditioning of the test samples under the uniaxial tension along, and perpendicular to, the direction of the fibers, shows a continuous softening and a decreasing hysteresis and stabilization for both directions.[57] After the initial preconditioning in the direction of the fibers, a softer transverse stress response is observed.[57] Further, it is apparent that with an increasing loading rate, the ultimate strength in association with the tissue stiffness increases.[57,58] For comparative purposes, we observed the mechanical properties of pelvic tissues from pregnant and postmenopausal women and animal models (Table 3).

When we compared the pregnant ewe perineal body with other pelvic organs of the pregnant human body and the animal models, we found that the perineal body was the most extensible part of the pelvic floor at low deformations. In contrast, under large deformations, the perineal tissue became stiffer with the stiffness comparable to cervix and higher than bladder, rectum, anal sphincter, or levator ani. The ultimate stress and ultimate strain of pregnant ewe perineal tissue are very close to other pelvic floor organs (vagina, uterus, bladder, cervix, rectum, anal sphincter, levator ani muscle).

When we compared the postmenopausal ewe perineal body with other postmenopausal pelvic organs, the perineal body was the most extensible part of the pelvic floor at low deformations. The stiffness in the large deformation region

TABLE 3. *Mechanical parameters of pelvic tissues of pregnant and postmenopausal women and animal models obtained from literature: the moduli of elasticity at small deformation region (E_0, MPa) and at large deformation region (E_1, MPa), respectively, ultimate stress (MPa), ultimate strain, and the mean age of donors*

Pregnant subjects	E_0	E_1	Ultimate strain	Ultimate stress	Animal model	Age	Ref.
Vaginal tissue	1.76	3.88	0.48	1.25	Ovine	3 y	[59]
	—	7.9	0.21	0.95	Rat	3 mos	[55]
	—	—	1.73	2.68	Rat	10 wks	[22]
	—	0.28	0.87	0.14	Mice	—	[58]
Proximal	5	18	0.27	3.5	Ovine	3 y	[56]
Distal	2.5	11	0.3	2.1	Ovine	3 y	[56]
Uterus	—	—	0.32	0.66	Human	—	[60]
Bladder	0.13	0.43	1.40	0.31	Ovine	3 y	[59]
Cervix	0.25	1.73	0.71	0.81	Ovine	3 y	[59]
	—	1	—	—	Ovine	—	[61]
Uterine end	—	0.91	—	—	Ovine	—	[61]
Mid cervix	—	1.06	—	—	Ovine	—	[61]
Vaginal end	—	1.07	—	—	Ovine	—	[61]
Rectum	0.11	0.36	1.14	0.40	Ovine	3 y	[59]
Anal sphincter	0.11	0.35	1.29	0.27	Ovine	3 y	[59]
Levator ani muscle	0.08	0.08	1.04	0.09	Ovine	3 y	[59]
Perineal body	0.04	1.12	0.98	0.58	Ovine	2 y	Current study
Postmenopausal subjects	**E_0**	**E_1**	**Ultimate strain**	**Ultimate stress**	**Animal model**	**Age**	**Ref.**
Vaginal tissue	0.39	1.49	—	—	Human	75 y	[62]
	0.35	1.32	—	—	Human	79 y	[63]
	—	15-32	0.4-0.7	3-7	Ovine	4-5 y	[64]
With prolapse	0.007				Human	47 y	[65]
	0.010				Human	43 y	[65]
	0.40-0.60	1.20-3.20	0.2	—	Human	75 y	[33]
	—	10.26	1.37	0.42	Human	60 y	[66]
With prolapse	—	12.10	0.39	0.27	Human	60 y	[66]
With prolapse	—	14.35	—	—	Human	69 y	[67]
Uterus		0.48-1.38		0.55-2.07	Human	–	[68]
Bladder	0.09	0.007	—	—	Human	75 y	[62]
	—	1.3		0.7	Human	50-65 y	[69]
	0.20-0.30	0.20-0.50	0.8	—	Human	75 y	[33]
Rectum	0.35	0.07	—	—	Human	75 y	[62]
	0.25-0.40	0.20-0.80	0.3	—	Human	75 y	[33]
Uterosacral ligament	0.83	5.70	—	—	Human	83 y	[62]
	1.56	10.39	—	—	Human	84 y	[70]
Round ligament	0.70	4.62	—	—	Human	83 y	[62]
	0.82	6.69	—	—	Human	84 y	[70]
Broad ligament	0.42	1.32	—	—	Human	83 y	[62]
	0.58	2.66	—	—	Human	84 y	[70]
Perineal body	0.02	0.23	1.40	0.17	Human	74 y	[27]
	0.03	1.75	0.87	0.63	Ovine	7 y	Current study

was similar to vaginal tissue and pelvic ligament stiffness. The ultimate stress of the perineal tissue was close to human bladder, uterus, and vaginal tissue. The ultimate strain of ewe perineal tissue was close to human bladder and ovine vaginal tissue.

Study limitations

This study has several limitations. We did not know the gross anatomy of the structures in the tissue samples obtained by, for example, MRI, to know the location of the perineal muscles and their insertions on the tendons. The results of measurements carried out in the open air could be influenced by dehydration of the tissue. The dehydration could lead to a slight stiffening of the tissue during experimentation.[71] However, this potential source of bias was minimized by the short duration of the experiments (about 15 minutes). We did not make blind assessments, but the specimens were evaluated in random manner not per groups to minimize an eventual evaluation bias.

Potential clinical value

The results can be used for improvement of mathematical models simulating delivery or pelvic floor dysfunctions, and POP. Computational modeling and simulation is nowadays important to overcome the hindrance in precise clinical measurement. In the clinical setting, it is impossible to precisely and timely measure the perineal strain at the time of its maximum, that is, at the time of fetal head expulsion, because this expulsion process lasts only 1 to 2 seconds. Furthermore, based on the current evidence, it would be unethical not providing manual perineal support. However, the execution of this support/placement of the hand on the perineum disallows any perineal measurement and makes obtaining true clinical data impossible. Moreover, the

situation is complicated by the number of variables needed to be taken into account: parity, maternal age, maternal BMI, fetal weight, fetal head dimensions, duration of the second stage of labor, instrumental delivery, episiotomy, maternal cooperation, perineal edema, perineal dimensions, perineal elasticity, dexterity and experience of the accoucheur, and so on. This all makes an exact and thorough clinical evaluation not feasible.

Computational modeling may help with many of those difficulties, allowing for a reliable repetition of a numerical experiment using the same parameters and changing just one or two variables, thus enabling adequate analysis of the chosen variable. For instance, we may use ''the same mother'' (identical maternal parameters) and change the position and movement of the fingers of the accoucheur during manual perineal protection thus analyzing this obstetrical intervention. The recent perineal computational models serving this purpose were limited regarding their material characteristics (unknown) and due to their homogeneous structure.

Our data ought to refine those models subsequently providing more precise analysis to achieve a more detailed navigation of the clinician in certain complex obstetrical situations.

CONCLUSIONS

In the present study, we identified the volume fractions of the smooth and skeletal muscles, elastin, type I collagen, and adipose cells of the ewe perineal body and the Young's moduli of elasticity, and the ultimate stress and strain of the ewe perineal bodies using a uniaxial tension loading. Our findings showed that the tissue stiffness depends on the level of loading with significant stiffening at strains higher than 18%. The ewe perineal body showed homogeneous tissue composition and mechanical properties across the sites of the perineal body. The perineal body of ewes during delivery had a higher amount of skeletal muscle tissue, a lower amount of type I collagen, and a higher Young's modulus of elasticity in the small deformation region when compared with this structure after ovariectomy.

The results regarding ewes during delivery can be used for improvement of mathematical finite element based models simulating delivery.[6-13] The results regarding ewes after ovariectomy can be used for models describing the behavior of the pelvic floor when simulating its dysfunctions or POP.[12,15-18,72]

The morphometric data, in the form of continuous variables, are made publicly available for biomechanical modeling of the perineal body, as shown in Supplementary material 2, http://links.lww.com/MENO/A445.

REFERENCES

1. Shafik A, El-Sibai O, Shafik AA, Shafik IA. A novel concept for the surgical anatomy of the perineal body. *Dis Colon Rectum* 2007;50:2120-2125.
2. Stoker J. Anorectal and pelvic floor anatomy. *Best Pract Res Clin Gastroenterol* 2009;23:463-475.
3. Schorge JO, Hoffman BL, Bradshaw KD, Halvorson LM, Schaffer JI, Corton MM, editors. *Williams Gynecology*, 3rd ed. New York: McGraw-Hill education; 2016.
4. Kovac SR, Zimmerman CW, editors. *Advances in Reconstructive Vaginal Surgery*, 2nd ed. Philadelphia: Wolters Kluwer Health/Lippincott Williams & Wilkins; 2012.
5. Walters MD, Karram MM, editors. Urogynecology and Reconstructive Pelvic Surgery. 3rd ed. Philadelphia: Mosby Elsevier; 2007.
6. Jing D, Ashton-Miller Ja, DeLancey JOL. A subject-specific anisotropic visco-hyperelastic finite element model of female pelvic floor stress and strain during the second stage of labor. *J Biomech* 2012;45:455-460.
7. Parente MPL, Natal Jorge RM, Mascarenhas T, Fernandes AA, Martins JAC. Deformation of the pelvic floor muscles during a vaginal delivery. *Int Urogynecol J Pelvic Floor Dysfunct* 2008;19:65-71.
8. Parente MPL, Natal Jorge RM, Mascarenhas T, Fernandes AA, Martins JAC. The influence of the material properties on the biomechanical behavior of the pelvic floor muscles during vaginal delivery. *J Biomech* 2009;42:1301-1306.
9. Lien K-C, DeLancey JOL, Ashton-Miller JA. Biomechanical analyses of the efficacy of patterns of maternal effort on second-stage progress. *Obstet Gynecol* 2009;113:873-880.
10. Li X, Kruger J, Chung J, Nash M, Nielsen P. Modelling childbirth: comparing athlete and non-athlete pelvic floor mechanics. *Med Image Comput Comput Interv* 2008;11:750-757.
11. Martins JAC, Pato MPM, Pires EB, Natal Jorge RM, Parente M, Mascarenhas T. Finite element studies of the deformation of the pelvic floor. *Ann N Y Acad Sci* 2007;1101:316-334.
12. Rostaminia G, Abramowitch S. Finite element modeling in female pelvic floor medicine: a literature review. *Curr Obstet Gynecol Rep* 2015;4:125-131.
13. Jansova M, Kalis V, Rusavy Z, Zemcik R, Lobovsky L, Laine K. Modeling manual perineal protection during vaginal delivery. *Int Urogynecol J* 2014;25:65-71.
14. Chanda A, Unnikrishnan V, Roy S, Richter HE. Computational modeling of the female pelvic support structures and organs to understand the mechanism of pelvic organ prolapse: a review. *Appl Mech Rev* 2015;67:040801.
15. Chen L, Ashton-Miller JA, DeLancey JOL. A 3D finite element model of anterior vaginal wall support to evaluate mechanisms underlying cystocele formation. *J Biomech* 2009;42:1371-1377.
16. Ren S, Xie B, Wang J, Rong Q. Three-dimensional modeling of the pelvic floor support systems of subjects with and without pelvic organ prolapse. *Biomed Res Int* 2015;2015:1-9.
17. Chen ZW, Joli P, Feng ZQ, Rahim M, Pirró N, Bellemare ME. Female patient-specific finite element modeling of pelvic organ prolapse (POP). *J Biomech* 2015;48:238-245.
18. Yang Z, Hayes J, Krishnamurty S, Grosse IR. 3D finite element modeling of pelvic organ prolapse. *Comput Methods Biomech Biomed Engin* 2016;5842:1-13.
19. Noakes KF, Bissett IP, Pullan AJ, Cheng LK. Anatomically realistic three-dimensional meshes of the pelvic floor and anal canal for finite element analysis. *Ann Biomed Eng* 2008;36:1060-1071.
20. D'Aulignac D, Martins JAC, Pires EB, Mascarenhas T, Natal Jorge RM. A shell finite element model of the pelvic floor muscles. *Comput Methods Biomech Biomed Engin* 2005;8:339-347.
21. Mayeur O, Lamblin G, Lecomte-Grosbras P, Brieu M, Rubod C, Cosson M. FE simulation for the understanding of the median cystocele prolapse occurrence. *Biomed Simul* 2016;44:220-227.
22. Jing D. *Experimental and theoretical biomechanical analyses of the second stage of labor*. The University of Michigan; 2010; PhD thesis.
23. Chen L, Low LK, DeLancey JOL, Ashton-Miller JA. In vivo estimation of perineal body properties using ultrasound quasistatic elastography in nulliparous women. *J Biomech* 2015;48:1575-1579.
24. Jing D, Lien K-C, Ashton-Miller JA, DeLancey JOL. Visco-elastic properties of the pelvic floor muscle in healthy women. In conference proceedings: Ashton-Miller JA, Hughes RE, Andrews D, editors. Ann Arbor, Michigan: North American Congress on Biomechanics; 2008, abstract no. 562, 1-2.
25. Baah-Dwomoh A, McGuire J, Tan T, De Vita R. Mechanical properties of female reproductive organs and supporting connective tissues: A review of the current state of knowledge. *Appl Mech Rev* 2016;68:060801.
26. Lee S, Darzi A, Yang G. Subject specific finite element modelling of the levator ani. *Med Image Comput Comput Assist Interv* 2005;8:360-367.
27. Kochová P, Cimrman R, Jansová M, et al. The histological microstructure and in vitro mechanical properties of the human female postmenopausal perineal body. *Menopause* 2019;26:66-77.

28. Abramowitch SD, Feola A, Jallah Z, Moalli P a. Tissue mechanics, animal models, and pelvic organ prolapse: a review. *Eur J Obstet Gynecol Reprod Biol* 2009;144(Suppl):S146-S158.
29. Patnaik SS, Borazjani A, Brazile B, et al. Pelvic Floor Biomechanics From Animal Models. Biomech Female Pelvic Floor 2016:131-48. doi: 10.1016/B978-0-12-803228-2.00006-4.
30. Urbankova I, Vdoviakova K, Rynkevic R, et al. Comparative anatomy of the ovine and female pelvis. *Gynecol Obstet Invest* 2017;82:582-591.
31. Jansova M, Kalis V, Rusavy Z, Räisänen S, Lobovsky L, Laine K. Fetal head size and effect of manual perineal protection. *PLoS One* 2017;12:e0189842.
32. Moon DK, Woo SL-Y, Takakura Y, Gabriel MT, Abramowitch SD. The effects of refreezing on the viscoelastic and tensile properties of ligaments. *J Biomech* 2006;39:1153-1157.
33. Rubod C, Brieu M, Cosson M, et al. Biomechanical properties of human pelvic organs. *Urology* 2012;79:968.e17–e22.
34. de Menezes Reiff RB, Croci AT, Neto RB, Pereira CAM. Comparative study on mechanical properties of the central portion of frozen and fresh calcaneus tendon. *Acta Ortopédica Bras* 2007;15:6-8.
35. Rubod C, Boukerrou M, Brieu M, Jean-Charles C, Dubois P, Cosson M. Biomechanical properties of vaginal tissue: preliminary results. *Int Urogynecol J Pelvic Floor Dysfunct* 2008;19:811-816.
36. Stemper BD, Yoganandan N, Pintar FA. Mechanics of arterial subfailure with increasing loading rate. *J Biomech* 2007;40:1806-1812.
37. Howard V, Reed M. Unbiased Stereology: Three-Dimensional Measurement in Microscopy (Advanced Methods). 2nd ed. New York, USA: Garland Science; 2005.
38. Mouton PR. *Principles and Practices of Unibiased Stereology: An Introduction for Bioscientists*. Baltimore, Maryland: Johns Hopkins University Press; 2001.
39. Shafik A, Ahmed I, Shafik AA, El-Ghamrawy TA, El-Sibai O. Surgical anatomy of the perineal muscles and their role in perineal disorders. *Anat Sci Int* 2005;80:167-171.
40. Tosun OC, Mutlu EK, Tosun G, et al. Do stages of menopause affect the outcomes of pelvic floor muscle training? *Menopause* 2014;22:175-184.
41. Kraima AC, West NP, Treanor D, et al. The anatomy of the perineal body in relation to abdominoperineal excision for low rectal cancer. *Colorectal Dis* 2016;18:688-695.
42. Fung YC. Biomechanics: Mechanical Properties of Living Tissues, 2nd ed. New York, USA: Springer-Verlag; 1993.
43. Alberts B, Johnson A, Lewis J, Raff M, Roberts K, Walter P, editors. Molecular Biology of the Cell, 4th ed. New York, USA: Garland Science; 2002.
44. Meyers MA, Chen P-Y, Lin AY-M, Seki Y. Biological materials: structure and mechanical properties. *Prog Mater Sci* 2008;53:1-206.
45. Vincent JF V. Structural Biomaterials, 3rd ed. Princeton, UK: Macmillan Education UK; 1982.
46. Kot BCW, Zhang ZJ, Lee AWC, Leung VYF, Fu SN. Elastic modulus of muscle and tendon with shear wave ultrasound elastography: variations with different technical settings. *PLoS One* 2012;7:e44348.
47. Lieber RL. *Skeletal Muscle Structure, Function and Plasticity: The Physiological Basis of Rehabilitation*, 3rd ed. USA: Wolters Kluwer/ Lippincott Williams & Wilkins: Baltimore, Maryland; 2002.
48. Gennisson J-L, Deffieux T, Macé E, et al. Viscoelastic and anisotropic mechanical properties of in vivo muscle tissue assessed by supersonic shear imaging. *Ultrasound Med Biol* 2010;36:789-801.
49. Mason P. Dynamic stiffness and crossbridge action in muscle. *Biophys Struct Mech* 1978;4:15-25.
50. Wuyts FL, Vanhuyse VJ, Langewouters GJ, Decraemer WF, Raman ER, Buyle S. Elastic properties of human aortas in relation to age and atherosclerosis: a structural model. *Phys Med Biol* 1995;40:1577-1597.
51. Zemčík R, Karbanova J, Kalis V, Lobovský L, Jansová M, Rusavy Z. Stereophotogrammetry of the perineum during vaginal delivery. *Int J Gynaecol Obstet* 2012;119:76-80.
52. Peña E, Martins P, Mascarenhas T, et al. Mechanical characterization of the softening behavior of human vaginal tissue. *J Mech Behav Biomed Mater* 2011;4:275-283.
53. Calvo B, Peña E, Martins P, et al. On modelling damage process in vaginal tissue. *J Biomech* 2009;42:642-651.
54. Cosson M, Lambaudie E, Boukerrou M, Lobry P, Crépin G, Ego A. A biomechanical study of the strength of vaginal tissues. *Eur J Obstet Gynecol Reprod Biol* 2004;112:201-205.
55. Feola A, Moalli P, Alperin M, Duerr R, Gandley RE, Abramowitch S. Impact of pregnancy and vaginal delivery on the passive and active mechanics of the rat vagina. *Ann Biomed Eng* 2011;39:549-558.
56. Rynkevic R, Martins P, Hympanova L, Almeida H, Fernandes AA, Deprest J. Biomechanical and morphological properties of the multiparous ovine vagina and effect of subsequent pregnancy. *J Biomech* 2017;57:94-102.
57. Ehret AE, Itskov M. Modeling of anisotropic softening phenomena: application to soft biological tissues. *Int J Plast* 2009; 25:901-919.
58. Rahn DD, Ruff MD, Brown Sa, Tibbals HF, Word RA. Biomechanical properties of the vaginal wall: effect of pregnancy, elastic fiber deficiency, and pelvic organ prolapse. *Am J Obstet Gynecol* 2008;198:590e1-e5906.
59. Rynkevic R, Martins P, Andre A, Parente M, Mascarenhas T, Almeida H, Fernandes AA. The effect of consecutive pregnancies on the ovine pelvic soft tissues: link between biomechanical and histological components. *Ann Anat* 2019;222:166-172.
60. Manoogian SJ, Bisplinghoff JA, Kemper AR, Duma SM. Dynamic material properties of the pregnant human uterus. *J Biomech* 2012; 45:1724-1727.
61. Owiny JR, Fitzpatrick RJ, Spiller DG, Dobson H. Mechanical properties of the ovine cervix during pregnancy, labour and immediately after parturition. *Br Vet J* 1991;147:432-436.
62. Chantereau P, Brieu M, Kammal M, Farthmann J, Gabriel B, Cosson M. Mechanical properties of pelvic soft tissue of young women and impact of aging. *Int Urogynecol J* 2014;25:1547-1553.
63. Gabriel B, Rubod C, Brieu M, Dedet B, de Landsheere L, Delmas V, Cosson M. Vagina abdominal skin, and aponeurosis: do they have similar biomechanical properties? *Int Urogynecol J* 2011;22:23-27.
64. Ulrich D, Edwards SL, Letouzey V, et al. Regional variation in tissue composition and biomechanical properties of postmenopausal ovine and human vagina. *PLoS One* 2014;9:e104972.
65. Epstein LB, Graham CA, Heit MH. Systemic and vaginal biomechanical properties of women with normal vaginal support and pelvic organ prolapse. *Am J Obstet Gynecol* 2007;197:165.e1-165.e6.
66. Lei L, Song Y, Chen R. Biomechanical properties of prolapsed vaginal tissue in pre- and postmenopausal women. *Int Urogynecol J* 2007;18:603-607.
67. Goh JT. Biomechanical properties of prolapsed vaginal tissue in pre- and postmenopausal women. *Int Urogynecol J Pelvic Floor Dysfunct* 2002;13:76-79.
68. Pearsall GW, Roberts VL. Passive mechanical properties of uterine muscle (myometrium) tested in vitro. *J Biomech* 1978;11:167-176.
69. Martins PA, Filho AL, Fonseca AM, et al. Uniaxial mechanical behavior of the human female bladder. *Int Urogynecol J* 2011;22:991-995.
70. Rivaux G, Rubod C, Dedet B, et al. Comparative analysis of pelvic ligaments: a biomechanics study. *Int Urogynecol J Pelvic Floor Dysfunct* 2013;24:135-139.
71. Viidik A. Biomechanical behavior of soft connective tissues. In Akkas N, editor. Prog. Biomech., Alphen Aan Den Rijn: Sijthoff & Nordhoff; 1979. pp. 75-113.
72. Chanda A, Unnikrishnan V, Roy S, Richter HE. Computational modeling of the female pelvic support structures and organs to understand the mechanism of pelvic organ prolapse: a review. *Appl Mech Rev* 2015;67.